Mechanisms of Development, 44 (1993) 189–207

MOD 00209

Altered *Pax* gene expression in murine notochord mutants: the notochord is required to initiate and maintain ventral identity in the somite

Susanne Dietrich, Frank R. Schubert and Peter Gruss *

Abteilung für Molekulare Zellbiologie, Max-Planck-Institut für Biophysikalische Chemie, Am Faßberg, D-37077 Göttingen, Germany

(Received 27 September 1993; accepted 9 October 1993)

We have characterised the patterning capacity of the notochord on the somite using the murine *Pax-1* gene as a ventral, and *Pax-3* as a dorsal molecular marker. As model systems we chose the four mouse notochord mutants *Brachyury curtailed* (T^c), *Danforth's short tail* (*Sd*), *Pintail* (*Pt*) and *truncate* (*tc*). Their notochord either is initially absent or progressively degenerates. The use of these mutants enabled us to compare the effect of graded notochord deficiencies. All four mutants show premature termination of the vertebral column. This phenotype can be traced back to an impaired dorsoventral specification of the somites. In *tc/tc* and $T^c/+$ embryos the notochord in the affected regions is missing from the beginning. Consequently, *Pax-1* is never activated, and *Pax-3* remains to be expressed in the entire somite. In contrast, in *Sd* and *Pt* embryos the notochord secondarily degenerates. At the end of the prevertebral column *Pax-1* expression is lost, while the *Pax-3* signal occupies the former *Pax-1* expressing zone. The altered *Pax* gene expression in the notochord mutants suggests that the notochord is required for two processes in the dorsoventral patterning of the somite: first the induction of ventral structures, and second the maintenance of the ventral fate.

Pax-1; Pax-3; T gene; Notochord; Somite; Dorsoventral patterning; Mouse mutant; *Brachyury curtailed; Danforth's short tail; Pintail; Truncate*

Introduction

The central skeletal element of vertebrates, the vertebral column, combines solidity, stability, elasticity and mobility, allowing the evolution of giants like dinosaurs or whales. The mechanical properties of the vertebral column are conferred by the metameric array of vertebrae which are separated by intervertebral discs in higher vertebrates and directly articulated in the lower vertebrate classes. Despite these differences, the principles of vertebrate axial skeleton formation are conserved.

The source for the vertebral column components is the paraxial mesoderm. Laid down during gastrulation as a mesenchyme flanking notochord and neuroectoderm, this tissue segments when discrete somites detach by epithelialisation. The skeletogeneous part of the somite, the sclerotome emerges via mesenchymal transformation. This mesenchyme condenses in a metameric fashion, first laterally to form the neural arches, later medially giving rise to the vertebral bodies and the intervertebral discs (reviewed in Töndury and Theiler, 1990). The somite also produces a second tissue, the dermomyotome, which will subdivide into dermatome and myotome to form dermis and skeletal muscle. With respect to their position, somite cells have to acquire a dorsolateral identity to become dermomyotome, whereas a ventromedial identity restricts them to the sclerotome lineage. Thus, the dorsoventral differentiation of the somite is the crucial step in the formation of the axial skeleton as a whole.

Evidence accumulated that the regional specification of the somite is strongly influenced by the notochord. In notochord ectomised amphibian neurulae and chick embryos the myotome expands, finally fusing beneath the neural tube (Kitchin, 1949; Teillet and Le Douarin, 1983). Depending on the stage of somite development, the sclerotome either degenerates or

* Corresponding author.

forms an unsegmented cartilage tube surrounding the spinal cord. Implantation of an ectopic notochord favours the differentiation of somitic tissue into cartilage, inhibiting the development of the dorsal muscle or dermis (Pourquié et al., 1993). This effect can be mimicked by the floor plate. Notochord manipulations also influence the dorsoventral patterning of the neural tube, the neuroectodermal axial organ. Notochord grafts are capable of inducing an ectopic floor plate and columns of motor neurons, whereas extirpation of the notochord abolishes floor plate differentiation (e.g. Placzek et al., 1990; van Straaten et al., 1985; Yamada et al., 1991). Again, the floor plate, once induced, can similarly exert the ventralising function. Both in neural tube and paraxial mesoderm the notochord is essential for the ventral developmental pathway.

The microsurgical experiments that laid the foundations for our present knowledge on the notochord–somite interaction described the effects following the complete removal or addition of the notochord. Notochord mutants of the mouse in contrast may serve as model systems to study the graded notochordal loss. Homozygous *Brachyury* (*T/T*) animals never develop any notochord proper (Chesley, 1935). In *T/+* heterozygotes a notochord is present in the trunk, but remains irregularly shaped and attached to the hindgut or spinal cord. In the tail no notochord is formed (Chesley, 1935; Grüneberg, 1963). Thus, the *Brachyury* mutant may represent initial absence of the notochord. *Truncate* (*tc*) homozygotes show sudden interruptions or premature termination of the notochord (Theiler, 1959). In the affected regions, the sclerotomes degenerate, the dermomyotomes of contralateral somites fuse and the neural tube lacks the floor plate, thus resembling the regionalised phenotype of chorda-ectomised *Ambystoma* (Kitchin, 1949). In *Danforth's short tail* (*Sd*) homozygotes, the notochord is formed but collapses during midgestation (Gluecksohn-Schoenheimer, 1945; Paavola et al., 1980). The embryos lack both vertebral column (Gluecksohn-Schoenheimer, 1945, for review see Grüneberg, 1963) and floor plate (Bovolenta and Dodd, 1991; Theiler, 1959) in their posterior body region, whereas in the anterior region the notochord degeneration leaves both vertebral column and neural tube almost unaffected. In *Pintail* (*Pt*) animals the notochord diminishes due to low mitotic rates (Berry, 1960). Since this process lasts until birth, only moderately affecting the skeleton (Grüneberg, 1963), this mutant exhibits the mildest case. Though primary cause and extent of the notochord deficiencies are different, all of the mutants have in common that the notochord is lost at certain stages of development, incompatible with the proper formation of vertebral components at least in the tail. Thus, they are useful tools to investigate the role of the notochord during vertebral column formation in vivo.

The identification of events that lead to the premature termination of the vertebral column requires appropriate markers, initially responding to notochord alterations. We chose the murine *Pax-1* and *Pax-3* genes as such markers because of several reasons: being transcribed at day 8.25 post coitum (pc) the *Pax-1* gene so far is the earliest marker solely for the ventral portion of the somite (this study). At day 9.5 pc it is expressed in the entire sclerotome, later restricted to the anlagen of the intervertebral discs (Deutsch et al., 1988). The *Pax-1* mutation *undulated* affects mainly the ventromedial portion of the axial skeleton (Balling et al., 1988; Grüneberg, 1963) arguing that the gene is required for the development of these structures. The undulated mutation has been demonstrated to reinforce the *Sd* phenotype (Grüneberg, 1953; Wright, 1947) suggesting the *Pax-1* expression depends on an intact axial mesoderm.

Contrary to *Pax-1*, the expression of the *Pax-3* gene is restricted to the dorsal aspect of both somite and neural tube (Goulding et al., 1991, 1993). The mouse *Pax-3* mutation *Splotch* demonstrates the importance of this gene for the development of dorsal structures, as the dorsally emerging neural crest cells are defective and the neural tube frequently fails to close (Auerbach, 1954). After notochord excision in chick embryos the *Pax-3* expression in the neural tube extends ventrally (Goulding et al., 1993). Thus, *Pax-3* can serve as an appropriate dorsolateral marker for the interaction of the notochord with somite and spinal cord.

In this study we addressed the patterning capacity of the notochord on the somite by investigating the behaviour of early molecular markers in different notochord mutants of the mouse. We determined the onset

Fig. 1. Skeletal preparations of wildtype and notochord mutant embryos at day 13.5 pc. (A,B) Wildtype animal, NMRI×B6D2 mating. C, notochord; V, vertebral body; P, pedicle of the neural arch; L1, first lumbar vertebra; S1, first sacral vertebra; Ca1, first caudal vertebra; arrowhead indicates last vertebral condensation at the position of Ca20. (C,D) $T^c/+$; vertebral column ends at the level of S4 (C) and S3 (D); notochord ends in the same region. (E,F) *Sd/+*. (E) Animal with NMRI background; vertebral column ends at S4. (F) Animal with C57BL/6 anchestors; last vertebra Ca7; notochord rudiment indicated by arrow. (G,H) *Sd/Sd*; vertebral column ends at L4, the notochord is absent. (I,J) *Pt/+*; last vertebra Ca11; note reduced notochord diameter compared to the wildtype embryo. (K,L) *Pt/Pt*; vertebral column ends at the level of Ca5, the notochord ends in the posterior thoracic region; rib anlage on L1. (M,N,O) *tc/tc* day 13.0 pc; vertebral column and notochord are interrupted posterior to Ca4 and are terminated after Ca11. (O) Higher magnification of (M); note the branched notochord termini (arrowhead). The scale bar in (A) represents 1330 μm for the lateral views (A,C,E,G,I,K,M), 650 μm for the ventral views (B,D,F,H,J,L,N), and 260 μm for the lateral view in (O).

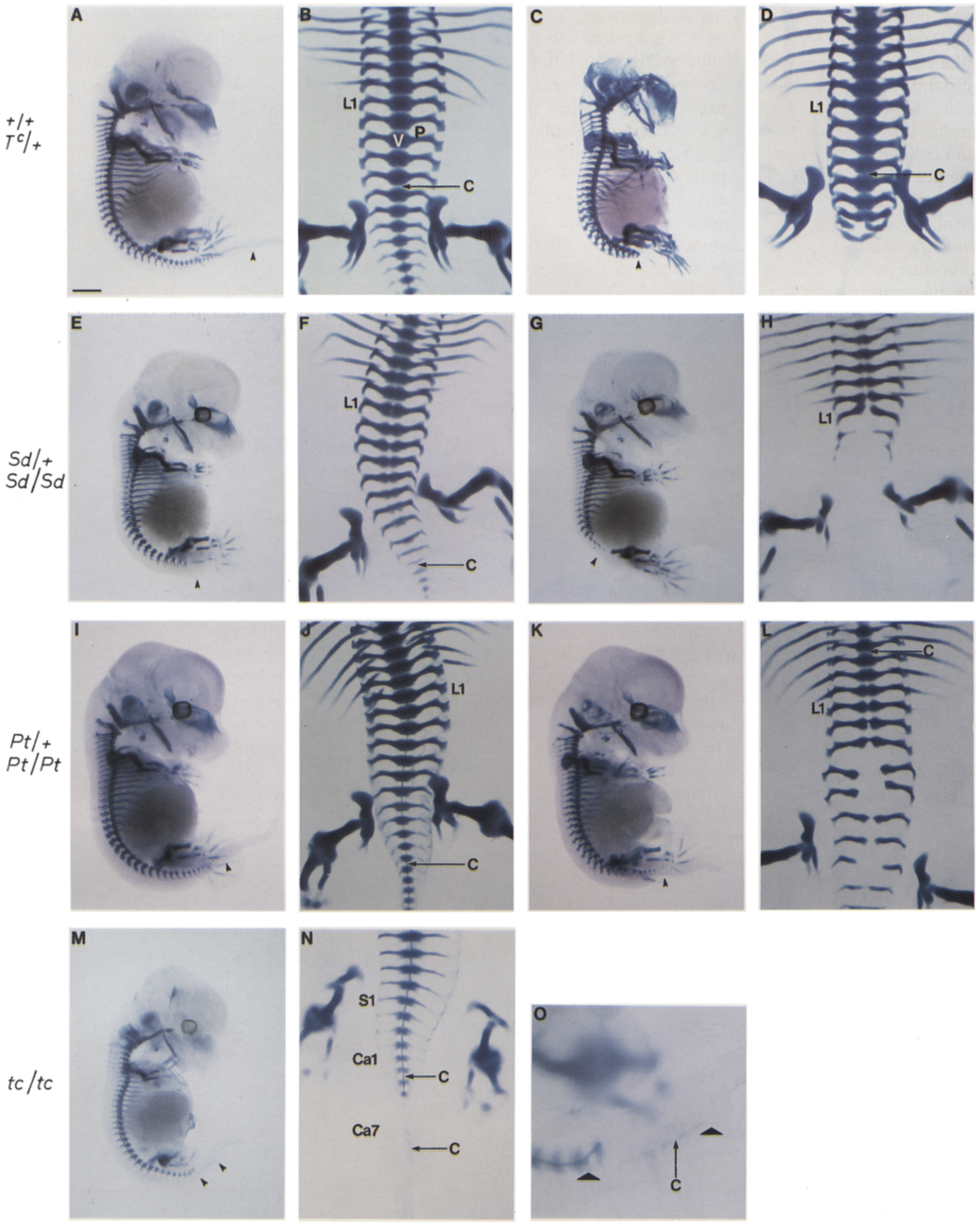
+/+
Tc/+
Sd/+
Sd/Sd
Pt/+
Pt/Pt
tc/tc
A
B
L1
V
P
C
D
L1
C
E
F
L1
C
G
H
L1
I
J
L1
C
K
L
C
L1
M
N
S1
Ca1
C
Ca7
C
O
C

and development of the *Pax-1* and *Pax-3* expression in the mutants *Brachyury curtailed* (T^c), *Danforth's short tail* (*Sd*), *Pintail* (*Pt*) and *truncate* (*tc*). The state of the notochord was analysed with a *T* antisense probe. In the posterior notochord-free regions the *Pax-1* staining is lost, correlating with the vertebral column phenotype. The *Pax-3* signal spreads ventrally in both somite and neural tube. The altered *Pax* gene expression pattern suggests a crucial role for the notochord in the dorsoventral patterning of the paraxial mesoderm.

Results

Phenotype of the notochord mutants at day 13.5 pc of embryonic development

In order to correlate the *Pax-1* expression pattern to the vertebral column phenotype, we analysed the skeleton of the four notochord mutants by alcian blue/alizarin red clearing preparation at day 13.5 pc of development. Animals of that age are developed far enough to have almost the entire axial skeleton preformed in cartilage, thus exhibiting the adult phenotype. Also, the skeletons are young enough to be related to the advanced *Pax-1* expression pattern at day 12.0–12.5 pc.

Wildtype embryos

In wildtype control animals obtained by NMRI × B6D2 mating or crosses of heterozygous mutants, averagely 53 vertebral bodies are represented by medial cartilage condensations (Fig. 1A,B). The anteriormost 30 vertebrae already show the anlage of the neural arch growing dorsad to surround the spinal cord. At the opposite end the vertebral condensations are not precisely defined yet. The notochord exceeds these

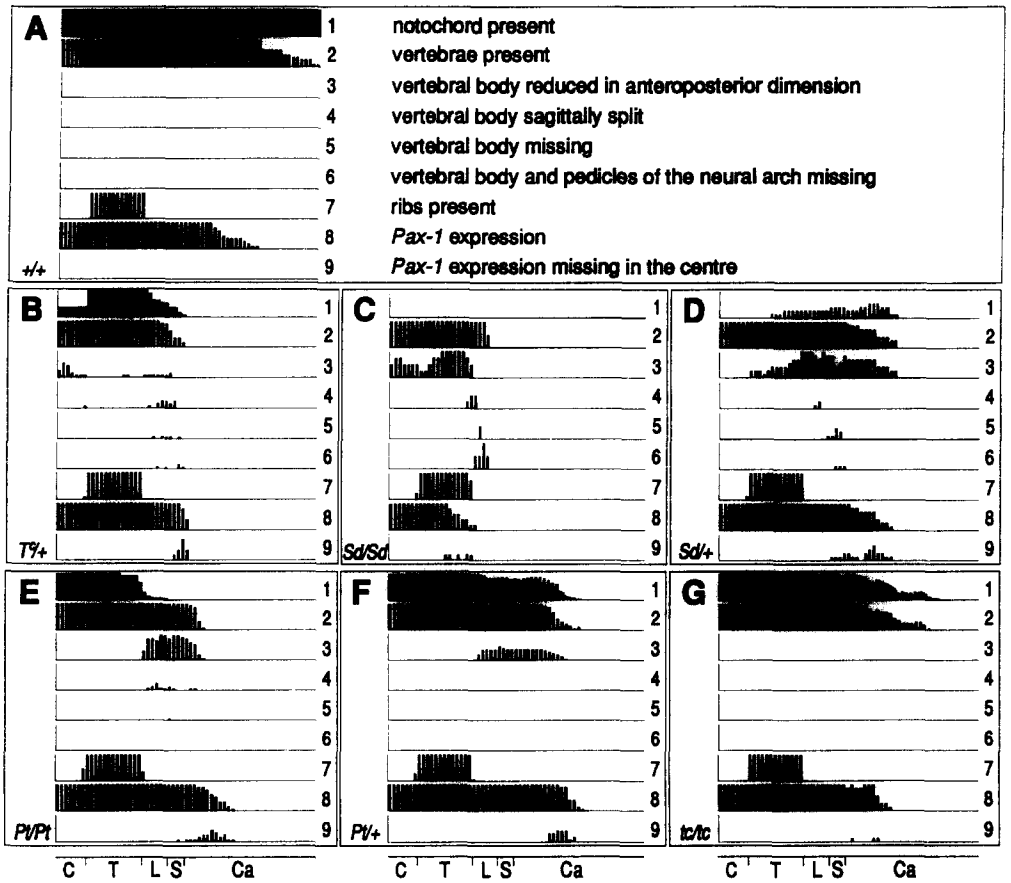

Fig. 2. Regional distribution of the mutant vertebral column phenotype and *Pax-1* expression along the longitudinal body axis. The skeletons of day (d) 13.5 pc animals were analysed for vertebral column length and presence of vertebral column components. The *Pax-1* expressing body segments were counted in d 11.5–12.0 pc embryos. To compare the data, they were normalised, calculating the total number of embryos in each category as 100%. Note that in *tc/tc* and $T^c/+$ mutants the length of the notochord correlates with the length of axial skeleton and the extent of the *Pax-1* expression. *Sd* and *Pt* animals are completely or partially deprived of the notochord. Vertebral column and *Pax-1* expression correlate, extending the length of the notochord rudiments. (A) Wildtype; d 13.5 pc, 11 embryos; d 11.5–12.0 pc, 10 embryos. (B) $T^c/+$; d 13.5 pc, 11 embryos; d 11.5–12.0 pc, 5 embryos. (C) *Sd/Sd*; d 13.5 pc, 4 embryos; d 11.5–12.0 pc, 5 embryos. (D) *Sd/+*; d 13.5 pc, 7 embryos; 3 NMRI background, 4 C57BL/6 background; d 11.5–12.0 pc, 7 embryos; 2 NMRI background, 5 C57BL/6 background. (E) *Pt/Pt*; d 13.5 pc, 15 embryos; d 11.5–12.0 pc, 11 embryos. (F) *Pt/+*; d 13.5 pc, 28 embryos; d 11.5–12.0 pc, 12 embryos. (G) *tc/tc*; d 13.5 pc, 16 embryos; d 11.5–12.0 pc, 7 embryos. C, cervical region; T, thoracic region; L, lumbar region; S, sacral region; Ca, caudal vertebral column.

condensations posteriorly indicating that 7–8 more caudal vertebrae have to be added.

Brachyury heterozygotes

Homozygous T^c/T^c embryos never reach the 13th day of development most likely because the allantois fails to contact the placenta (Gluecksohn-Schoenheimer, 1944). Therefore, only heterozygous $T^c/+$ animals are represented in the litters. They can be recognised by the absence of the caudal axial skeleton (Fig. 1C,D). The lumbar vertebral bodies may be reduced in their anteroposterior dimension. Within the 1–3 terminal vertebrae, this phenotype progressively increases leading to median split vertebrae, absence of the vertebral bodies and, in addition, the pedicles, or terminally to unstructured cartilage condensations. In the entire affected region, the lateral portions of the vertebrae may be fused. The vertebral phenotype reflects the situation of the notochord which stops up to 3 segments anterior to the last vertebra. The rostral notochord is represented by small nuclei pulposi. These may even be absent cervically explaining the reduction or absence of the dens axis in 50% of the animals. In one case the atlas was fused to the base of the skull. Previously reported rib fusions (Searle, 1966) did not occur in our stock, an additional rib rudiment on the cervical vertebra C7 was observed once.

Danforth's short tail

Homozygous *Sd/Sd* fetuses can be distinguished from their heterozygous littermates by the absence of the sacral and caudal vertebral column causing a flattened body shape (Fig. 1G,H). The cervical vertebrae show anteroposterior reductions including the loss of the dens axis. Sagittally split vertebrae occur in the lower thoracic and upper lumbar skeleton, followed by vertebral anlagen lacking the vertebral body or in addition the pedicles; the terminal vertebrae may be represented by amorphous lateral cartilage condensations. Posterior to the thorax the rudimentary vertebral bodies as well as the pedicles may fuse to their neighbours. In the case the split vertebra phenotype extends into the thoracic vertebral column, the ribs may be disconnected from the vertebra or completely absent indicating that the entire ventral aspect of the skeletogenous tissue is affected. Unlike $T^c/+$, no notochord is visible at all.

The phenotype of $Sd/+$ heterozygotes highly depends on the genetic background. Animals outcrossed to NMRI form 30–37 (Fig. 1E), those with C57BL/6

Fig. 3–7 (pp 194–195). Expression pattern of *Pax-1*, *Pax-3* and *T* in wildtype and mutant embryos; lateral view. The terminal *Pax-1* signal is labelled with an closed arrowhead. In some animals, staining reagents were trapped in the brain vesicles.

Fig. 3. Expression of the marker genes in wildtype embryos. (A) Onset of *Pax-1* expression at day (d) 8.25 pc. So, recently formed somite. *Pax-1* expression at d 10.5 pc (B) and d 12.0 pc (C). The axial staining is restricted to the sclerotomal part of the somites. S, sclerotome; F, forelimb bud; H, hindlimb bud. (D) *Pax-3* expression at d 11.5 pc. Along the longitudinal axis *Pax-3* is transcribed in the dermomyotome and the dorsal portion of the neural tube. D, dermatome; N, neural tube. (E) The *T* gene at d 11.5 pc is expressed in the tailbud and the notochord. T, tail bud; C, notochord.

Fig. 4. Marker gene expression in *Brachyury* embryos. (A) *Pax-1* expression in $+/+$ (left) and T^c/T^c (right) embryos at d 9.5 pc. Note the single *Pax-1* island posterior to the pericardium. (B) *Pax-3* expression in $+/+$ and T^c/T^c embryos at d 9.5 pc. Note the *Pax-3* staining in 7 mesodermal patches and the intense labelling of the posterior neuroectoderm. (C) Expression of the *T* gene in $+/+$ and absence of *T* staining in T^c/T^c embryos at d 9.5 pc. (D) T^c/T^c embryo at d 11.0 pc expressing *Pax-1* in one patch of paraxial mesoderm (arrowhead) and the dorsally shifted forelimb bud. Termination of the *Pax-1* staining in $T^c/+$ embryos posterior to the hindlimb bud at d 10.5 pc (E) and d11.5 pc (F). (G) *Pax-3* expression in $T^c/+$ embryo at d 12.0 pc. Note the ventrally extended *Pax-3* signal in neural tube and paraxial mesoderm posterior to the hindlimb bud (arrow). (H) *T* expression in $T^c/+$ embryos at d 12.0 pc is only found in some islands at the tip of the tail (arrow).

Fig. 5. Marker gene expression in *Danforth's short tail* embryos. *Pax-1* expression in *Sd/Sd* homozygotes is terminated at the level of the hindlimb bud at d 10.0 pc (A) and anterior to the hindlimb bud at d 12.0 pc (B). (C) *Sd/+* animal at d 12.0 pc. *Pax-1* is expressed normally in the trunk declining in the anterior region of the tail. (D) In *Sd/Sd* embryos at d 12.0 pc the *Pax-3* expression expands ventrally at the level of the hindlimb bud. Two arrows indicate the ventral shift first in the neural tube, and subsequently in the somite. (E) *T* staining in *Sd/Sd* embryos at d 12.0 pc is restricted to the tailbud (arrow).

Fig. 6. Expression of marker genes in *Pintail* embryos. Termination of *Pax-1* expression in *Pt/Pt* embryos at d 10.5 pc posterior to the hindlimb bud (A) and at d 12.0 pc in the anterior region of the tail (B). (C) In *Pt/+* embryos at d 12.0 pc the *Pax-1* signal is absent in the terminal somites of the tail. (D) *Pt/Pt* embryos at d 12.0 pc. Note the broadened mesodermal *Pax-3* staining in the posterior region of the tail (arrow). (E) *Pt/Pt* embryos at d 12.0 pc express the *T* gene in the tailbud and a short notochordal protrusion (arrow).

Fig. 7. Marker gene expression in *tc/tc* homozygotes. (A) Interrupted *Pax-1* staining at the level of the 8th somite at d 9.0 pc. (B) Higher magnification of (A). (C) Interruption of *Pax-1* expression in the tail of a *tc/tc* embryo at d 11.5 pc. (D) *Pax-3* pattern at d 12.0 pc. Two arrows indicate zones of widened mesodermal *Pax-3* staining. (E) *T* expression at d 12.0 pc. Note the gaps within the notochordal signal.

The scale bar in Fig. 3A represents 240 μm in Fig. 3A, 870 μm in Figs. 3B, 4D,E, 5A, and 6A, 1000 μm in Figs. 3C–E, 4F–H, 5B–E, 6B–E, and 7C–E, 400 μm in Figs. 4A,B, and 7A, 475 μm in Fig. 4C, and 100 μm in Fig. 7B.

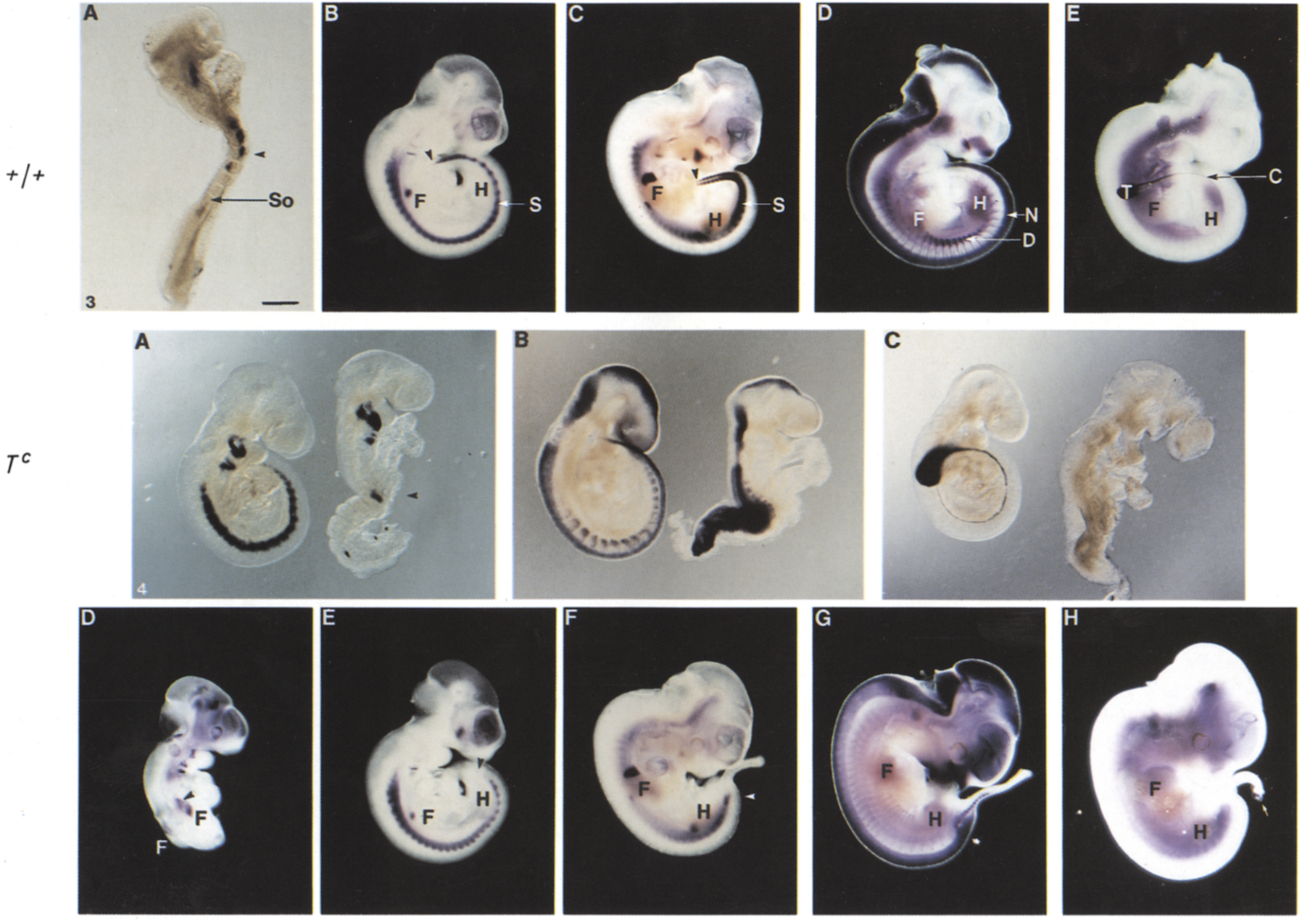
+/+
A
So
3
B
F
H
S
C
F
H
S
D
F
H
N
D
E
T
F
H
C
T^c
A
4
B
C
D
F
F
E
F
H
F
F
H
G
F
H
H
F
H

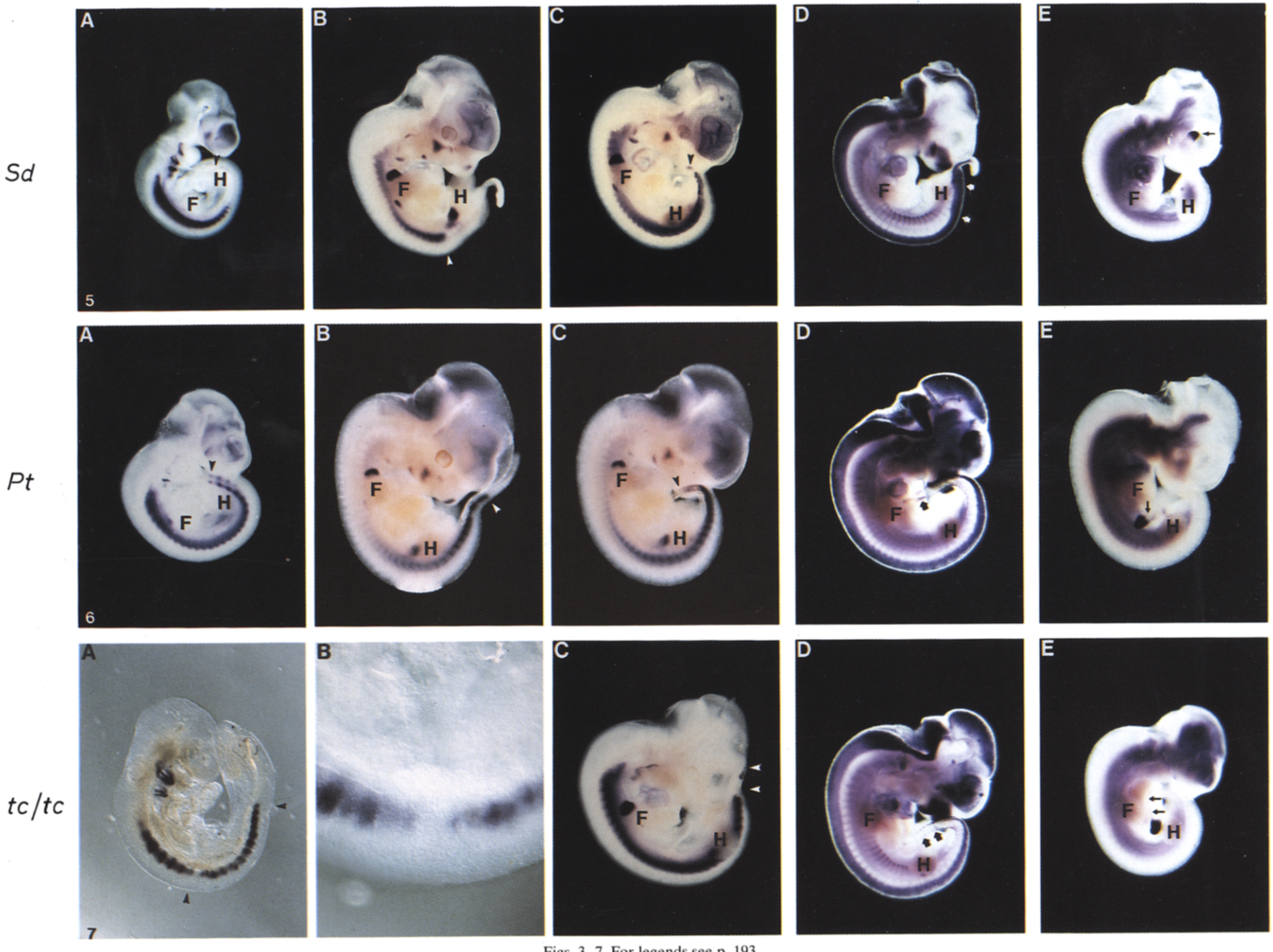

Figs. 3–7. For legends see p. 193.

ancestors 37–42 vertebrae (Fig. 1F). In the latter, the spine is more mildly affected. The upper vertebral column of both *Sd/+* classes resembles homozygotes including loss of the dens axis. In the lower portion, split vertebrae are less frequent. Absence of vertebral components occurred in 14% of the embryos, concentrated at the sacral vertebral column. From the thoracic region down to the caudal limit, stretches of notochord are present but reduced in diameter. In both, homozygous and heterozygous condition, a cervical rib on C7 was observed once.

Pintail

As denoted in Fig. 2, additional ribs are a common feature of *Pt* mutant mice. Compared to T^c and *Sd*, the overall phenotype of *Pt* animals is weaker (Fig. 1K,L). In *Pt/Pt* embryos up to 35 vertebrae are found. Malformations are concentrated on the lumbosacral region, where the vertebrae may be reduced or split, or may lack the vertebral body. Absence of the pedicles never was observed. The notochord can be depicted as a thin and fragile structure consecutively loosing diameter towards the posterior end. In the sacral region the notochord vanishes completely.

Also in *Pt/+* heterozygotes the thickness of the notochord is reduced in anteroposterior fashion (Fig. 1I,J). Nevertheless it still reaches the 16th caudal vertebra although the course may be interrupted several times. Vertebrae are found up to this position at most showing anteroposterior reductions.

Truncate homozygotes

In *Brachyury Curtailed* animals, *Sd* and *Pt* mutants, the phenotype increases steadily towards the caudal limit, never reaching the number of 53 vertebrae already preformed in the wildtype controls. With regard to these features, truncate animals differ significantly. Due to the incomplete penetrance of the mutation, homozygotes, in this study one animal out of 16, may appear perfectly normal. Phenotypically conspicuous embryos exhibit sudden interruptions or premature termination of the vertebral column leaving the remainder intact (Fig. 1M,N,O). The vertebral phenotype parallels the gaps within the notochord. In 19% of the animals, the notochord ended in an knoblike swelling and continued several segments later accompanied by vertebral condensations. Further 19% terminated the notochord in a dorsad curve, and in 25% of the embryos the notochord ended as a branch. The reappearing notochord may represent either the ventral or the dorsal course, may be reduced in diameter and may end again in one of the described structures. Though the notochordal interruptions can be observed at any position along the axis, they accumulate in the tail. Therefore the axial skeletons vary in length, in the animals investigated at day 13.5 pc ranging from 35 to 50 vertebrae.

The analysis of the mutant axial skeleton is summarised in Fig. 2 revealing that all mutations lead to vertebral column malformations either by a sudden or progressive loss of vertebral substance. Consequently, the *Sd/Sd* animals bear approximately 24, $T^c/+$ 27, *Pt/Pt* 33, *Sd/+* 37, and *Pt/+* 41 vertebrae. Also the average of truncate homozygotes develops 41 vertebrae, but the axial skeleton may be interrupted anteriorly. Nevertheless, since the notochordal phenotype is of different origin, different effects on the expression of the *Pax-1* gene/*Pax* genes can be investigated.

Expression of T, Pax-1 and Pax-3 in wildtype embryos

T: expression in tailbud and notochord

The murine *T* gene is transcribed as gastrulation begins (Wilkinson et al., 1990). During the days 8.5–12.0 pc included in this study, expression can be found in the primitive streak and in the tailbud, additionally in the head process and in the notochord (Figs. 3E and 4C). The staining fits with the idea of *T* labelling the stem cell population as well as its medial derivatives (Wilson et al., 1993).

Pax-1: expression in the ventral somite epithelium and sclerotome

The murine *Pax-1* gene is expressed as early as day 8.25 pc before the embryo enters the process of turning (Fig. 3A). Animals of that age already have formed up

Fig. 8. Spatial distribution of *Pax-1* transcripts at different axial levels. (A–F) Wildtype embryo at day (d) 11.5 pc. (A) Cross-section at the level of the hindlimb bud and (B) frontal section posterior to the hindlimb bud; D, dermatome; M, myotome; S, sclerotome; C, notochord; Sp, spinal ganglion; P, floor plate; in (B) anterior is left. *Pax-1* is expressed in the entire sclerotome, strongest in its lateral portion. Spinal nerves and intersegmental vessels are not stained. (C) Tail, dorsal view. The two youngest somites are *Pax-1* negative. Arrowhead indicates the recently formed somite (So). (D–F) Cross-sections towards the end of the tail showing the sclerotomal *Pax-1* expression in the fifth but one somite (D), the onset of *Pax-1* in the epithelial second last somite (E), and the absence of *Pax-1* staining in the newly formed somite (F); E, tail gut endoderm. (G) Cross-section of a wildtype embryo at day 9.0 pc. Note the *Pax-1* expression in the just deepithelialising somite. T^c/T^c, embryos at d 8.5 pc expressing (H) and at. d 9.0 pc not expressing *Pax-1* (I). (J–L) $T^c/+$ embryo at d 11.5 pc. Loss of *Pax-1* expression towards the posterior margin of the hindlimbs; notochord and floor plate visible only in (J). (M–O) *Sd/Sd* embryo at d 11.5 pc, Loss of *Pax-1* expression at the hindlimb level. The notochord is absent, floor plate present in (M). (P–R) *Pt/Pt* embryo at d 11.5 pc. Slow reduction of *Pax-1* signal in the tail, note light staining in (R). Small notochord present in (P,Q). (S–U) *tc/tc* embryo at d 11.5. Serial sections in the tail, note the signal pausing in (T). (A,B,D–F,J–R) Vibratome sections, 30 μm; (G–I,S–U microtome sections, 8 μm. (A,D–U) Cross-sections. The scale bar in (A) represents 100 μm in (A–C,J–O), and 50 μm in (D–I,P–U).

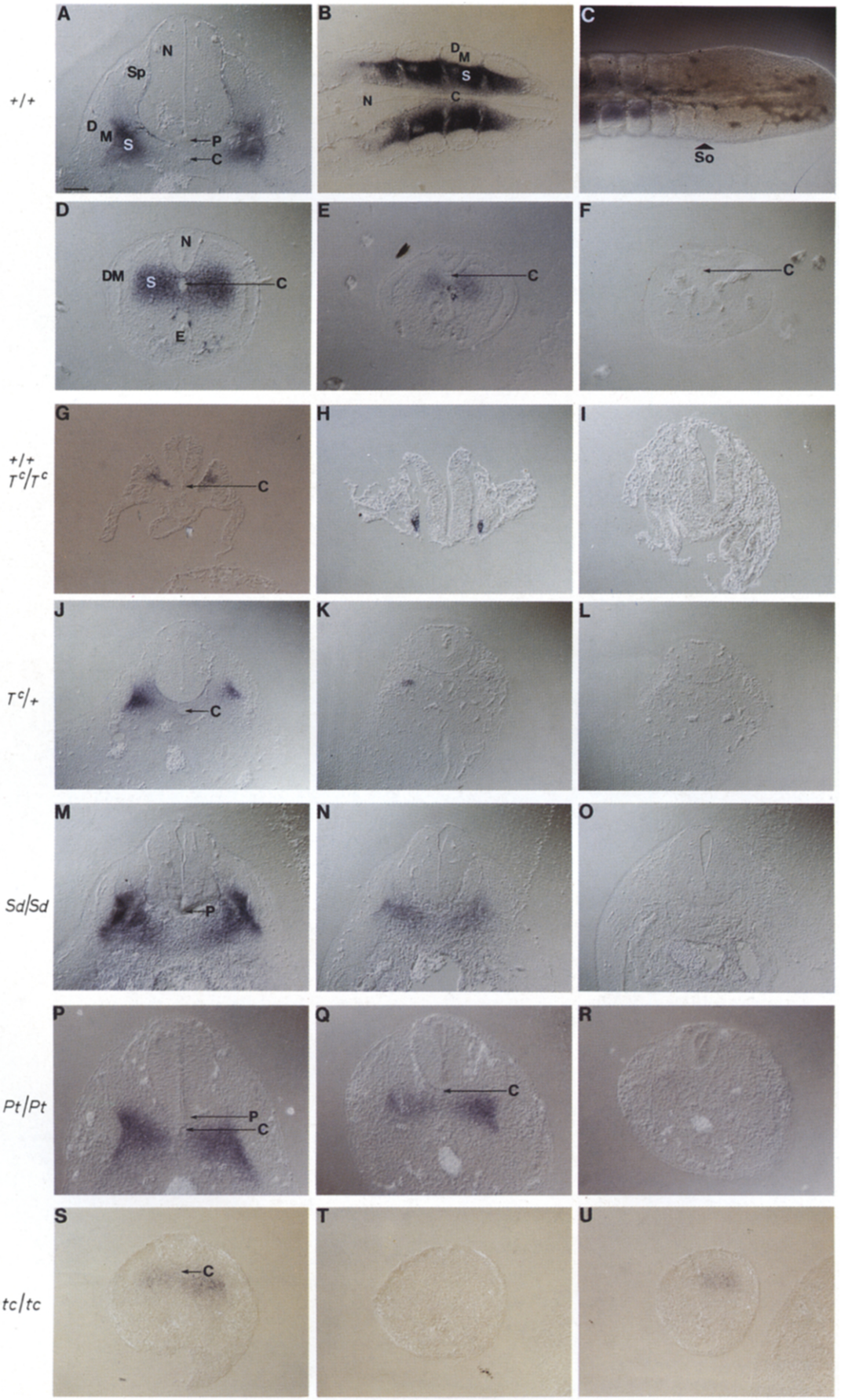
+/+
A
N
Sp
D
M
S
P
C
B
D
M
S
N
C
C
So
D
N
DM
S
C
E
E
C
F
C
+/+
Tc/Tc
G
C
H
I
J
Tc/+
C
K
L
M
Sd/Sd
P
N
O
P
Pt/Pt
P
C
Q
C
R
S
tc/tc
C
T
U

TABLE 1

Time course of the *Pax-1* expression

Genotype	No. of embryos: no. of *Pax-1* expressing segments/total no. of visible segments [1] at								No. of vertebrae at day 13.5pc
	d 8.5 pc	d 9.0 pc	d 9.5 pc	d 10.0 pc	d 10.5 pc	d 11.0 pc	d 11.5 pc	d 12.0 pc	
+/+	6: 6/10	7: 11/14	14: 19/22	9: 25/27	9: 34/36		6: 37/39	4: 44/45	53 = Ca23
T^c/T^c [2]	3: 2pp, 1 sp	12: 3pp			4: 1pp				none
T^c/+					13: 29/35		4: 29/38	1: 28/40	27 = S1
Sd/Sd			9: 21/26		2: 23/34		5: 17/n.d.		24 = L4
Sd/+ [3]					3: 35/37		2: 32/39 (N)		33 = Ca3 (N)
							5: 38/42 (C)		40 = Ca10 (C)
Pt/Pt					4: 29/32		11: 38/46		33 = Ca3
Pt/+					7: 30/31		12: 43/45		41 = Ca11
tc/tc		19: 14/17		6: 24/25	8: 29/31		7: 39/41		41 = Ca11

[1] Starting from day 10.5 pc only the trunk and tail segments were counted.
[2] pp and sp refer to the maximum no. of paired and single patches, respectively.
[3] Animals on NMRI (N) or C57BL/6 (C) background differ slightly in the phenotype.

to 7 somites. The anteriormost ones transcribe *Pax-1* in their ventromedial portions just before deepithelialisation, whereas the youngest 3–4 somites do not. This observation suggests *Pax-1* to be an early, but possibly not the first marker for the sclerotomal portion of the somite.

As the animals grow, consecutively adding segments to their body axes, more units turn on the *Pax-1* gene (Table 1). Thus, mouse embryos at day 9.5 pc express the gene in 19 out of 22 somites indicating the critical period for the formation of the cervical and thoracic vertebral column (Fig. 4A). At day 10.0 pc the lumbar, and at day 10.5 pc the lower sacral/upper caudal vertebral column is reached (Fig. 3B). At that stage, the anteriormost *Pax-1* signal is located in the head mesoderm as well as the base of the skull probably after the occipital somites lost their segmental array. Posteriorly, the compact dermomyotome still allows the identification of individual units. Therefore, from day 10.5 pc onwards only the segments in trunk and tail were counted. At day 11.5 pc *Pax-1* is expressed in 37 out of 39 body segments and at day 12.0 pc in 44 out of 45 units revealing that the number of nonexpressing somites decreases during development (Fig. 3C).

As the *Pax-1* expression progresses caudad, also the qualitative aspects of the *Pax-1* pattern change in anteroposterior manner (Fig. 8A–G). Starting from the ventromedial edge of the somite, the staining spreads towards the midline where the sclerotome forms the perichordal tube, and dorsad as the lateral sclerotome surrounds the spinal cord. Since the topology of axial components differs in trunk and tail (Griffith et al., 1992), the overall progression of the signal on cross-sections appears mediodorsad in the former and horizontal in the latter, giving rise to a triangular or trapezoid pattern. In any case, the myotome and possibly a very dorsal or lateral portion of the sclerotome remain *Pax-1* negative on both cross- and frontal sections.

From day 9.0 pc onwards, the signal within one somite converts into a less stained cranial and a more intensely labelled caudal portion anticipating the differentiation of the lateral sclerotome into a less cell dense anterior and a condensed posterior half (Figs. 3B and 7A,B). Approximately two days later, this process is repeated in the medial sclerotome restricting the *Pax-1* expression to the more cell dense anlage of the intervertebral disc. Since the latter takes place within the interior of the embryo, it can be followed by

Fig. 9. Spatial distribution of *Pax-3* transcripts at different axial levels. (A–F) Wildtype embryo at day (d) 11.5 pc. (A) Cross-section at the level of the hindlimb buds, abbreviations as in Fig. 8. (B) Frontal section, same orientation as Fig. 8B. *Pax-3* expression is restricted to the dermatome. (C) Tail, dorsal view. Note the signal in the tailbud, T, and the recently formed somite (So; arrowhead). (D–F) Cross-sections towards the end of the tail showing the *Pax-3* expression in the neural tube and in the dermomyotome of the fourth but last somite (D), the retreating *Pax-3* signal in the second but last somite (E), and the weak overall staining in the newly formed somite (F). (G) Cross-section of a wildtype embryo at day 9.0 pc. Note the restriction of *Pax-3* to the dermomyotome in the deepithelialising somite. (H) Cross-section and (I) dorsal view of a T^c/T^c embryo at d 9.5 pc. Note the mesodermal *Pax-3* signal and the enhanced expression in the neural tube, however not extending to the midline. (J–L) T^c/+ embryo at d 11.5 pc. Ventral expansion of *Pax-3* expression at the level of the hindlimbs; notochord and floor plate visible only in (J). The slightly stained circular stucture below the neural tube probably represents neural tissue. (M–O) *Sd/Sd* embryo at d 11.5 pc. Course of the *Pax-3* expansion between the hindlimb bud and the base of the tail. Note that in (O) the staining fuses below the neural tube. (P–R) *Pt/Pt* embryo at d 11.5 pc. Expression of *Pax-3* widens in the tail, not reaching the midline. (S–U) *tc/tc* embryo at d 11.5. Broadening of the *Pax-3* signal in the tail, note the overall expression in (U). (A,B,D–F,J–U) Vibratome sections, 30 μm; (G,H) microtome sections, 8 μm. (A,D–H,J–U) Cross-sections. The scale bar in (A) represents 100 μm in (A–C,I–O), and 50 μm in (D–H,P–U).

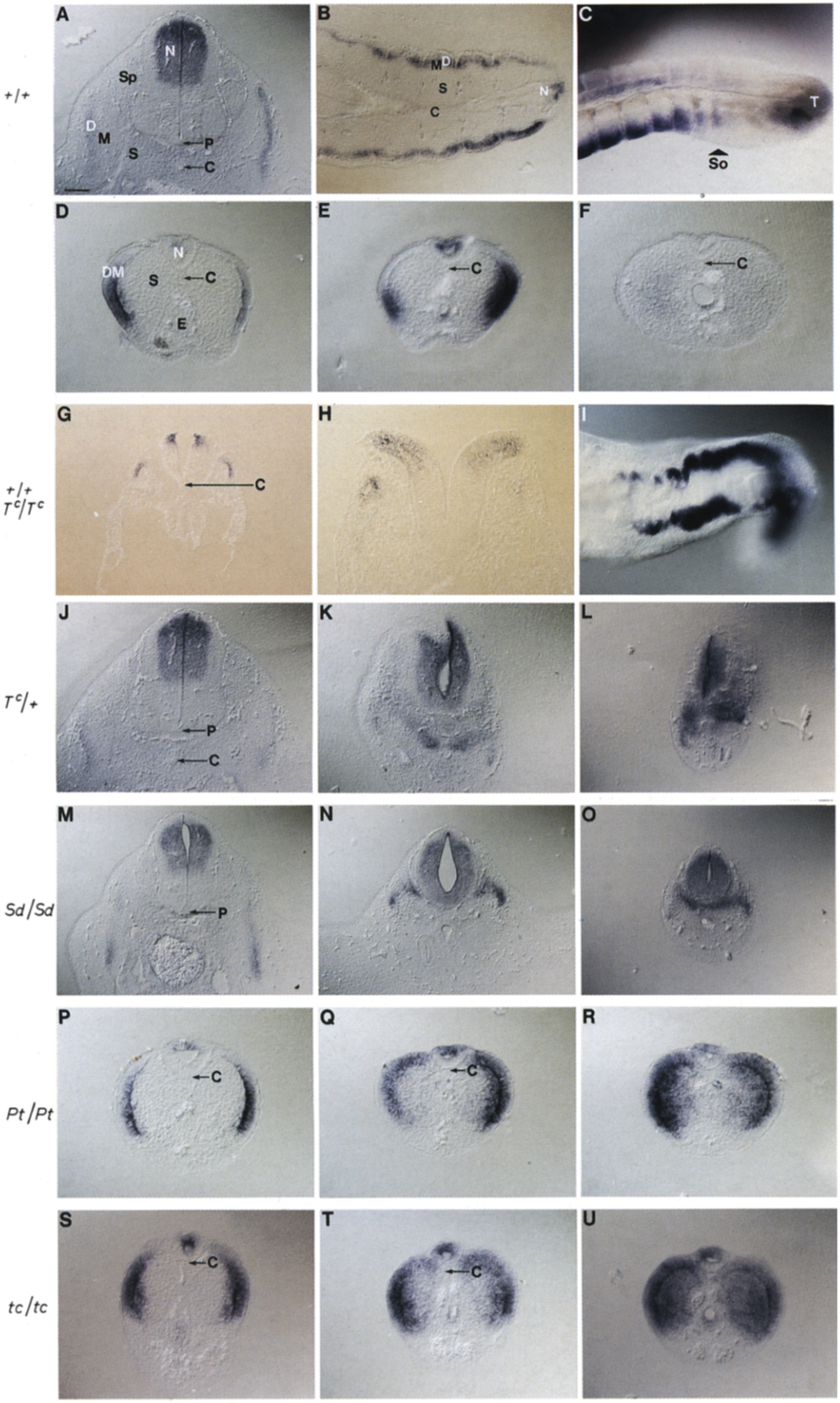
+/+
A
N
Sp
D
M
S
P
C
B
D
M
S
C
N
C
T
So
D
N
DM
S
C
E
E
C
F
C
+/+
Tc/Tc
G
C
H
I
Tc/+
J
P
C
K
L
Sd/Sd
M
P
N
O
Pt/Pt
P
C
Q
C
R
tc/tc
S
C
T
C
U

whole mount in situ hybridisation just when the tail region is reached at day 13.5 pc. Besides the axial skeleton, the *Pax-1* gene is successively activated in the pharyngeal pouches from day 8.25 pc onwards (Figs. 3A, 4A, 3B), in the forelimb bud at day 10.5 pc (Fig. 3B), and at day 11.5 pc simultaneously in the hindlimb bud and face (Fig. 3C). These domains serve as additional landmarks and criteria to stage the embryos.

Pax-3: expression in the recently formed somite, dermomyotome and dorsal neural tube

The *Pax-3* gene is already expressed during gastrulation in the primitive streak (Goulding et al., 1993) and subsequently in the tailbud (Fig. 9C). Later, expression is found briefly in the tail gut endoderm. The neuroectodermal staining can be observed first in the neural fold before closure (Fig. 4B). After the neural canal has formed, the signal occupies the dorsal half of the ventricular zone (Fig. 3D, 9A). In the tail, probably due to the process of secondary neurulation (Griffith et al., 1992), the dorsal staining can be seen after the central lumen has developed (Fig. 9D–F). The paraxial mesoderm weakly expresses *Pax-3* as somites are formed (Fig. 9F), in the trunk following the onset in the neural tube, in the tail simultaneously with the neuroectodermal *Pax-3* activation. In both regions the somites transcribe *Pax-3* prior to *Pax-1*. First distributed throughout, the staining simultaneously becomes enhanced and restricted to the dorsal dermomyotome, when the *Pax-1* expression occupies the prospective sclerotome (Fig. 9C–E). In intact animals as well as on cross- and frontal sections, the signal appeared as a blue cap sitting on top of the sclerotome, most intensely labelled at the posterolateral margin. As the myotome separates from the dermatome, *Pax-3* becomes restricted to the dermatome (Fig. 3D, 9A–G).

Like for the *Pax-1* gene, *Pax-3* expression traverses the entire embryo throughout the longitudinal axis. In contrast to the former, *Pax-3* is restricted to dorsolateral structures, in the mesoderm separated from *Pax-1* by a nonexpressing zone. Interestingly, at day 11.5 *Pax-3* expression can be found in the face overlapping with the *Pax-1* staining (Fig. 3D).

Expression of marker genes in Brachyury curtailed (T^c) mutant embryos

T expression in T^c

To obtain homozygous embryos, heterozygotes were mated inter se. T^c/T^c embryos can be identified by the creased neuroectoderm that often fails to close, the distended pericardium, and the absence of the allantois (Searle, 1966). They die around day 11.0 pc. As reported for the T^{wis} allele (Herrmann, 1991), the T^c/T^c homozygotes neither at day 9.0 pc (Fig. 4C) nor at day 11.0 pc express the *T* gene. Heterozygotes of that age indistinguishably from +/+ animals show a strong staining in the primitive streak/tailbud and the notochord. At day 12.0 pc $T^c/+$ embryos can be recognised by the filamentous tail. They do not exhibit any midaxial staining except the extreme tailbud. In cases the tail tip was swollen or branched, the *T* pattern was divided into corresponding islands (Fig. 4H).

Pax-1 expression in T^c

Using external shape and *Pax-1* expression as criteria, homozygous T^c/T^c embryos are conspicuous already at day 8.25–8.5 pc and day 9.0–9.5 pc. Though no distinct somites visible, up to 3 paired *Pax-1* signals were found beside the neural tube (Fig. 4A). In one case, a further *Pax-1* positive island was added unilaterally indicating that both halves of the embryo can be affected differently. Cross-sections (Fig. 8H) demonstrate the staining to be mesodermal, residing on both sides of the neuroectoderm. Neither notochord nor floor plate are detectable by morphological means. In the posterior body region, no *Pax-1* staining was observed (Fig. 8I). Since the *Pax-1* expression in the pharyngeal pouches appears normal, mainly axial organs seem to be involved in the mutant phenotype. At day 10.5–11.0 pc four embryos were analysed. Two did not stain at all, probably due to beginning resorption. One expressed *Pax-1* exclusively in the pharyngeal pouches. The largest homozygote had developed dorsally shifted forelimb buds showing the usual *Pax-1* signal (Fig. 4D). Anteriorly, a medial paired staining was detected also, indicating that axial *Pax-1* expression is principally possible until the timepoint of death.

Heterozygous $T^c/+$ animals differ from their wild-type littermates first at day 10.5–11.0 pc: the most advanced embryos begin to develop tail restrictions. The *Pax-1* staining is limited to 29 out of 35 body segments (Table 1). The 2–5 posteriormost signals appear less intense lacking the ventral portion (Fig. 4E). As in the later stages, the nonaxial *Pax-1* expression domains are not affected. At day 11.5 pc the heterozygotes can clearly be identified because of the filamentous tail (Fig. 4F). Twenty-nine out of 38 body segments express *Pax-1*. The terminal signals are weak and may just consist of small spots located in the posterior half of the somite. In one case the last but one was almost undetectable. Cross-sections (Fig. 8J–L) demonstrate that the light staining is due to a stepwise reduction of the *Pax-1* expressing zone both dorsolaterally beside and ventromedially below the neural tube, parallelling the loss of a morphologically defined notochord and floor plate, respectively. Most pronounced is the $T^c/+$ phenotype at day 12.0 pc. From the 40 segments visible, the anterior 28 are *Pax-1* positive whereas 12 units do not stain, implying that somites added to the body axis fail to turn on the *Pax-1* gene.

Pax-3 expression in T^c

The *Pax-3* expression was investigated starting at day 9.5 pc. Among 3 T^c/T^c embryos, one showed 3 lateral paired signals anterior to the heavily kinked region, one exhibited 8 patches of that kind (Fig. 4B), and one restricted its 2 patches to the left side. In all cases the neural tube except the midline was strongly stained (Fig. 9H,I), indicating an expansion of dorsal identity. At day 11.0 pc, the homozygous embryo analysed manifested staining in 4 paired patches anterior and 2 patches posterior to the rectangular body kink. In anteroposterior dimension, the *Pax-3* islands were not clearly separated. The spinal cord expression resembled the pattern at day 9.0 pc.

$T^c/+$ heterozygotes express *Pax-3* indistinguishably from wildtype embryos at day 9.5 pc. At stage 11.0–12.0 pc the *Pax-3* domain extends in the same proportion as the *Pax-1* staining becomes narrowed: up to the 27–28th body segment the *Pax-3* pattern appears unaltered; the following 14–18 somites show a broadened signal covering the segment entirely (Fig. 4G). In one animal the terminal 4 somites seemed pyknotic lacking the *Pax-3* expression. The neural tube staining occupies the ventromedial half at the level of the 28–30th segment. It stops 1–6 somites further posteriorly. On cross-sections (Fig. 9J–L), the *Pax-3* domains are dorsally restricted where notochord and floor plate are visible, ventrally expanding further posterior: first enhanced dorsomedially, the mesodermal signal aligns the neural tube, most likely not touching the remaining *Pax-1* spots; finally it fuses at the midline. Earlier than in the somite, the ventral extreme is reached within the neural tube. Below, a spherical structure with epithelially arranged cells is found. Since this tissue shows on some sections continuity with the neural tube and slightly stains with the *Pax-3* probe, it might represent a branch of this organ rather than an enlarged notochord as speculated earlier (reviewed in Töndury and Theiler, 1990). In all of the mutant animals, the tailbud remains negative for *Pax-3*, whereas the nonaxial expression domains resemble the wildtype situation.

Analysis of marker gene expression in Danforth's short tail (Sd) animals

T expression in Sd

Embryos obtained from heterozygote mating were examined from day 8.5–9.0 pc onwards. Among ten animals, one did not show any signal posterior to the branchial arch level except in the tailbud. It is not clear whether this animal represents an *Sd/Sd* homozygote, since at day 10.5 pc the 2 animals with the most limited expression still exhibited a fragile and narrow notochordal staining from the anterior margin to the middle thoracic/upper lumbar region. Two more mildly affected animals, most likely *Sd/+*, lacked the *T* signal only at the cranial/cervical level; in the thorax the staining appeared normal becoming faint and fragile from the lumbosacral region to the caudal limit. Two littermates strongly expressed *T* throughout the axis, thus believed to be +/+. At day 11.5–12.0 pc, the phenotypically defined *Sd/Sd* apart from the tailbud do not express *T* (Fig. 5E), whereas in *Sd/+* animals an interrupted blue line was left in the tail. The consecutive loss of *T* expression most likely reflects earlier observations that, starting at day 9.5 pc the notochord disappears until day 11.5 pc in homozygous *Sd/Sd*, and from day 10.0 pc to the time of birth in the heterozygotes (Gluecksohn-Schoenheimer, 1945).

Pax-1 expression in Sd

With regard to the *Pax-1* expression, *Sd/Sd* mutant embryos can first be identified at day 9.5–10.0 pc. In 9 animals, averagely 21 out of 26 body segments showed *Pax-1* signals (Table 1), the last 3–6 appearing less intense and lacking the medial portion (Fig. 5A). Eighteen littermates exhibited the wildtype pattern expressing *Pax-1* in 27 out of 28 body segments. As in the later stages, all embryos share the same unaltered expression pattern in pharyngeal pouches and limb buds. Since the number of animals did not fit the 1:2:1 ratio, allocation of heterozygotes to the first group cannot be excluded. At day 10.5–11.0 pc the homozygotes are phenotypically conspicuous because of the beginning tail restriction. They express *Pax-1* in the anterior 23 of 34 body segments. Again, the caudalmost 7 signals appear weak; the last 4 may be represented by small dots only, located in the posterior portion of the somite. In one case, the weakly stained units were preceded by 9 nonexpressing ones. At day 11.5–12.0 pc, the 5 homozygous *Sd/Sd* could clearly be identified because of the short dorsally bent tail filament and a low grade spina bifida (Fig. 5B). Compared to the day before, the axial *Pax-1* expression is even more restricted, terminating at the 20th-21st body segment. In one case, 14 *Pax-1* positive segments were followed by 5 negative and 5 weakly expressing somites. Cross-sections (Fig. 8M–O) demonstrate the consecutive loss of *Pax-1* staining as described for $T^c/+$ animals. A notochord is not visible, whereas a floor plate is present on the anteriormost sections accompanied by the normal *Pax-1* pattern.

Heterozygous *Sd/+* animals can first be identified at day 10.5–11.0 pc. They show a more moderately restricted *Pax-1* pattern than the homozygotes, expressing the gene in 35 out of 37 body segments (Table 1). Throughout the trunk the signal appears normal, decreasing in the tail. At day 11.5–12.0 pc tail restriction has begun, more prominent in *Sd/+* with NMRI background (Fig. 5C). These animals express *Pax-1* on average in 32 of 39 somites, the last 4–5 signals being

weak and sometimes fused laterally. Embryos with C57BL/6 ancestors show staining in 38 of 42 segments probably explaining the elongated tails observed in the skeletal preparations.

Pax-3 expression in Sd

The *Pax-3* experiments in *Sd* recalled the observations made in T^c: expansion of the *Pax-3* domain parallels the restriction of *Pax-1* expression. At day 10.0–11.0 pc the animals express the *Pax-3* gene in all body segments. In 3 animals, supposedly *Sd/Sd*, the terminal 7–8 signals appeared broadened. Posterior to the 16th–21st segment, the spinal cord expression is shifted towards the midline. Staining in the tailbud could not be observed. In 9 animals the terminal 2–4 units showed a widened *Pax-3* expression; the tailbud signal was absent. These embryos may represent the heterozygous condition.

At stage 11.5–12.0 pc 3 *Sd/Sd* were analysed. The mesodermal *Pax-3* expression both in whole embryos (Fig. 5D) and on the sections (Fig. 9M–O) appeared normal for the anterior 20–25 segments. In the terminal 13–18 it shifted ventrally along the walls of the neural tube, finally joining at the midline. In one case, the last 2 adjacent signals had fused laterally giving up their segmental array. The staining in the neural tube lost the dorsal restriction already from the 15–24th position onwards preceding the alteration in the somites. Two of the animals did not express *Pax-3* in the posterior portion of the tail probably due to tissue degeneration. The tailbud never was stained and the notochord absent throughout. Nevertheless, in the anterior region of the neural tube the typical floor plate structure was visible.

Marker gene expression in Pintail (Pt) embryos

T expression in Pt

The *T* expression was analysed in homozygous *Pt/Pt* animals starting at day 9.0–9.5 pc. At that stage, the *T* signal is already lost cranially and faint in the cervical region. No staining could be detected at day 12.0 pc except in the tailbud and a narrow notochordal projection (Fig. 6E), contrasting the presence of notochordal structures in the skeletal preparations. Therefore, *T* expression might be a marker exclusively for an intact notochord.

Pax-1 expression in Pt

Comparing litters obtained from $Pt/+ \times Pt/Pt$ and $Pt/Pt \times Pt/Pt$ matings, no differences were found before day 10.5 pc. At that stage, the homozygotes on average express *Pax-1* in 29 out of 32 body segments (Table 1, Fig. 6A). Up to 7 terminal somites are either weakly labelled or fail to express. At day 11.5–12.0 pc *Pt/Pt* mutants do not express *Pax-1* in about the last 8 somites, only the anterior 38 body segments being positive (Fig. 6B). Especially in cases of few non-expressing somites, the terminal signals appear weak, lacking the ventral and anterior aspect. Prior to the caudal limit, the staining may pause for 1–2 units. Cross-sections of this zone (Fig. 8P–R) reveal that the remaining signals are compressed to small spots half way between midline and surface ectoderm. The notochord is visible only as a tiny circle and vanishes on the last section. At the developmental stage of the affected region, presence or absence of the floor plate cannot be decided by morphological means. In any case, the number of *Pax-1* expressing somites exceeds the number of axial skeletal elements found at day 13.5 pc, providing the idea that stepwise reduction of notochordal tissue causes the loss of activating and maintaining signals necessary for *Pax-1* expression.

Heterozygotes at day 10.5 pc transcribe *Pax-1* in 30 out of 31 units (Table 1). At most 3 segments are weakly stained, 2 may remain blank. At day 11.5–12.0 pc *Pt/+* embryos exhibit *Pax-1* staining in 43 out of 45 trunk somites (Fig. 6C). Thus, they do not significantly differ from the wildtype controls as expected for a vertebral column phenotype starting at the 41st vertebra.

Pax-3 expression in Pt

Corresponding to the *Pax-1* experiments, at day 9.5 pc the *Pax-3* expression pattern does not differ among homozygous *Pt/Pt* and wildtype animals. At day 11.5–12.0 pc, the paraxial mesoderm expresses the gene down to the caudal limit; the last 5–6 signals appear broadened, progressively giving up their restriction to the posterolateral margin of the segment (Fig. 6D). Cross-sections (Fig. 9P–R) demonstrate that in this region the expression is extended ventrally both in the somite and the neural tube. In contrast to the more strongly affected mutants, the midline is not reached even when the notochord is invisible.

Expression of marker genes in truncate (tc/tc) homozygotes

T expression in tc/tc

Expression of the *T* gene was tested in 2 *tc/tc* animals of stage 12.0 pc. The first one exhibited a strong signal only in the tailbud. The notochord was occasionally visible, represented by a tiny line. In the second embryo the *T* signal appeared slightly thinner than in wildtype animals, showing brief discontinuities within the tail notochord (Fig. 7E). Thus, the 2 animals may represent the gross variation in truncate mutant phenotype.

Pax-1 expression in tc/tc

Opposite to *Sd* and *Pt*, in *tc/tc* animals the *Pax-1* expression in most cases is abruptly altered. At day

8.5–9.5 pc, the 19 *tc/tc* embryos appeared normal (Table 1) except for one that failed to express *Pax-1* within the 8th somite (Fig. 7A,B). At day 10.5–11.0 pc one embryo showed a faint staining within the 21st-23rd body segment, surrounded by 29 normally labelled units. Another animal expressed the gene in the anterior 30 trunk somites, followed by a blank one, a blue spot on the left side, 2 further negative units, 2 normal ones and a left terminal patch. Eleven littermates appeared completely normal. At day 11.5–12.0 pc, 2 embryos of 7 displayed interruptions of *Pax-1* expression along the axis. The more strongly affected animal expressed the gene normally in 30 body segments and weakly in the adjacent 31st. The signal paused for 2 units and reappeared for another 2 normally and 1 weakly stained one, leaving the last 2 somites blank (Fig. 7C). The second animal lacked the *Pax-1* signal in the 39–40th and in the terminal 42nd-46th somite.

The distribution of *Pax-1* negative somites at all stages of vertebral column formation suggests that the truncate mutation causes punctual rather than cumulative alterations of the axial skeleton. This idea is supported by the cross-sections on the day 9.0 pc and day 11.5 pc embryos. Within 30 μm the *Pax-1* signal vanishes completely, reappearing posteriorly (Fig. 8S–U). In the *Pax-1* negative zone no notochord can be found.

Pax-3 expression in tc / tc

The *Pax-3* expression pattern was analysed in 4 *tc/tc* mutant animals of stage 12.0 pc. Two exhibited staining in 40 of 42 and 41 of 44 body segments, respectively. One animal expressed *Pax-3* in all 42 units, the terminal 3 appearing broadened. In the 4th embryo all 46 body segments were labelled. A widened pattern can be observed within the 41st-42nd unit (Fig. 7D). The neural tube signal disappears posterior to the 39th trunk somite. In cross-sections, the expansion of *Pax-3* expression in both neural tube and paraxial mesoderm may reach the midline (Fig. 9S–U). On those sections no notochord is present. The effect is already seen in epithelialised somites suggesting that the notochordal influence is required at the latest soon after the somite has formed.

Discussion

Two systems of regional specification determine the development of the somites in vertebrates: one is the establishment of positional identity along the anteroposterior axis, conferred by the *Hox* code (Kessel and Gruss, 1991); the other is the subdivision of each individual unit in mediolateral (Ordahl and Le Dourain, 1992), anteroposterior and dorsoventral direction (reviewed in Töndury and Theiler, 1990). The dorsoventral differentiation leads to the formation of the dorsal and lateral dermomyotome destined to produce dermis and muscle, and the ventromedial sclerotome, which will give rise to all the vertebral components. Thus, the dorsoventral patterning of the somite initiates the vertebral column formation as a whole.

For a long time, the notochord has been suspected to be responsible for the development of ventral structures both in the somite and in the neural tube (e.g. Kitchin, 1949; van Straaten et al., 1985; Pourquié et al., 1993). To study the effects of different notochord deficiencies, we chose four mouse notochord mutants as model systems: *Brachyury curtailed* (T^c), *Danforth's short tail* (*Sd*), *Pintail* (*Pt*), and the recessive *truncate* (*tc*). In all of this mutants the notochord is lost to a different extent resulting in the premature termination of the vertebral column.

Anatomical studies on the mutant phenotypes pointed out that the loss of the posterior axial skeleton is preceded by sclerotome degeneration (Berry, 1960; Chesley, 1935; Gluecksohn-Schoenheimer, 1945; Theiler, 1959), suggesting that the notochord is required for the survival of this tissue. Alternatively, sclerotomal cells may die because they have not been properly instructed. This interpretation is supported by transplantation experiments in chicken that demonstrate the ventralising function of the notochord (Placzek et al., 1990; Pourquié et al., 1993; Yamada et al., 1991). To characterise the role of the notochord, we used the murine *Pax-1* and *Pax-3* genes as early molecular markers. *Pax-3* expression is initiated directly after somitogenesis, weakly labelling the entire somite. The signal enhances but simultaneously retracts to the dorsolateral aspect of the somite as *Pax-1* transcription begins ventromedially. Both genes are active prior to somite deepithelialisation, thus distinguishing different regions even before they appear morphologically distinct.

In the four mouse notochord mutants *Pax-1* expression is lost at the end of the prevertebral column. The *Pax-3* domain extends ventrally, in extreme cases occupying the entire somite. The dorsal identity is widened at the expense of the ventral, suggesting the notochord to produce a ventralising signal. Degeneration of the somitic mesenchyme is therefore interpreted as a secondary process following the impaired dorsoventral specification of the somite. However, it cannot be excluded that *Pax-1* is required to support cell proliferation as observed in tissue culture experiments (Maulbecker and Gruss, 1993).

Truncate and Brachyury: agenesis of the notochord prohibits the development of ventral identity

The individual alterations of marker gene expression correlate with the kind of notochord phenotype. In truncate animals, the vertebral column at any axial

level may be suddenly interrupted or terminated, precisely parallelling gaps within the notochord. The *T* signal shows as sudden interruptions illustrating pauses in notochord formation. Similarly, the *Pax-1* expression disappears abruptly; only somites directly flanking the gaps may exhibit less intense staining. The *Pax-3* signal expands as rapidly, strongly labelling the entire somite. The changes in *Pax* gene expression can be traced back to the epithelially arranged somite; *Pax-1* is not activated whereas the weak overall *Pax-3* staining enhances without becoming dorsolaterally restricted. Therefore, the somite retains its original specification, indicating that directly after somitogenesis the notochord is required to ventralise the paraxial mesoderm. In chicken, addition or removal of the notochord at the level of the segmental plate suggests a ventralising influence of the axial mesoderm even before somite formation (Pourquié et al., 1993). In any case, the initial absence of the notochord is incompatible with the activation of *Pax-1* and the initiation of the ventral developmental pathway within the presumably dorsally predisposed paraxial mesoderm.

In $T^c/+$ animals both vertebral column and notochord end in the sacral region. In cases the notochord does not reach the terminal vertebrae, they lack the ventromedial components. *T* expression is restricted to some islands at the tip of the tail reflecting the defective tailbud (Wilson et al., 1993). Consequently, structure and marker gene expression in tailbud derived tissues are affected: while anteriorly expressed in wild-type fashion, *Pax-1* sacrally declines within 1–3 segments. Simultaneously, the *Pax-3* staining expands, not touching the remaining *Pax-1* spots. In this intermediate zone, notochord and floor plate are absent by morphological means; the neural tube may be branched. At any stage of development the *Pax-1* expression ends after 29 segments, suggesting that the reduced *Pax-1* staining is a result of insufficient induction. The tail entirely lacks the spinal cord. *Pax-3* is expressed throughout the paraxial mesoderm as observed in the notochord-less regions of *tc* embryos, illustrating the dorsal specification of this tissue. Thus, failure of notochord formation in the $T^c/+$ tail results in the failure of somite ventralisation and in subsequent absence of the caudal vertebral column.

Homozygous T^c/T^c embryos are believed not to develop any notochord at all (Searle, 1966) as suggested by the absence of *T* expression at day 9.5 pc. Furthermore, they do not form somites which could be recognised as discrete blocks flanking the neuroectoderm. However, in the anteriormost body regions *Pax-1* and *Pax-3* are expressed in condensed mesodermal patches at the usual ventral or dorsal position. Posteriorly, only *Pax-3* staining is found, not joining at the midline. Also in the heavily bent neural tissue the *Pax-3* signal leaves out the ventral extreme, though a floor plate is absent by morphological means. Thus, T^c/T^c embryos might still be able to form dispersed axial mesoderm not expressing *T* but retaining some notochordal activity.

Danforth's short tail and Pintail: notochord degeneration prevents the maintenance of the ventral paraxial mesoderm

In *Sd/Sd* animals a notochord is formed but degenerates completely between day 9.5 and 11.0 pc as indicated by the restriction of *T* expression to the tailbud. The vertebral column, though deprived from the notochord, extends to the lumbar region, the last 3–5 vertebrae lacking the ventromedial components. The *Pax* gene expression pattern anticipates the three-partite vertebral column phenotype. In the anterior body region even though the notochord is absent, the marker genes are expressed normally and the floor plate is established in the neural tube. Transplantation experiments show that the floor plate is able to mimic the ventralising function of the notochord (Placzek et al., 1990; Pourquié et al., 1993; Yamada et al., 1991). In *Sd/Sd* homozygotes the floor plate may similarly substitute the notochord function. Alternatively, after somite and neural tube have sufficiently developed, notochord alterations may not affect them any more. At the prospective posterior end of the axial skeleton *Pax-1* is not activated, whereas *Pax-3* strongly labels both somite and neural tube. This pattern corresponds to the one observed in notochord-free regions of *tc/tc* embryos indicating that the notochord disappeared before ventrality was induced.

The intermediate thoracolumbar zone is characterised by two properties: the *Pax-1* gene is expressed but becomes progressively restricted to small patches located halfway between surface ectoderm and spinal cord in the caudal portion of the somite; in the same proportion the *Pax-3* staining expands. Prior to the changes observed in the paraxial mesoderm, the *Pax-3* domain widens within the neural tube while the floor plate is absent. Thus, similar to $T^c/+$, the degenerating notochord fails to properly establish ventral identity. Encompassing 7 segments at day 10.0–10.5 pc, the intermediate zone becomes compressed to 3 units as *Pax-1* is turned off posteriorly. Apparently different from $T^c/+$, the number of *Pax-1* positive segments declines during development, approaching the number of vertebrae found at day 13.5 pc. *Pax-3* occupies the *Pax-1* deprived mesoderm indicating that the tissue became dorsalised. Thus, within a time window the regional specification of axial tissues can be reprogrammed. In this period the notochord is required to maintain ventral identity.

In Pintail mice the notochord progressively looses diameter. At day 11.5 pc the *T* probe only labels the

tailbud and a thin notochordal projection, suggesting that the notochord rudiments found on sections and at day13.5 by skeletal preparation are defective. More similar to *Sd/+* heterozygotes, the notochord diminishes slowly, allowing the development of an axial skeleton even in the upper caudal region. At the cervical and thoracic level, *Pax* gene expression and vertebrae appear completely normal. Posteriorly, the *Pax-3* staining is moderately widened at the expense of the *Pax-1* signal corresponding to the mild reduction of vertebrae within this zone. The number of 38 *Pax-1* positive body segments at day 11.5–12.0 pc contrasts 33 vertebral anlagen at day 13.5 pc, supporting the idea that the notochord is needed to maintain ventral quality.

The mutant skeletal phenotypes correlate with reduction of Pax-1 expression

The mouse notochord mutants demonstrate the effects of the various notochord deficiencies on the paraxial mesoderm, displayed by the altered *Pax* gene expression. Absence of the notochord before somitogenesis prevents ventralisation of the somite, retaining its initial dorsal specification. A later, progressive notochordal loss results in a partly or even complete secondary dorsalisation of already ventrally specified cells, the extent depending on the time point of notochord degeneration. The broadening of the mesodermal *Pax-3* domain starts as a ventral expansion in the regions flanking the neural tube. The *Pax-1* expression ceases proportionally, residing longest within lateral islands (Fig. 10A). Either the events along the midline enclose the distal parts of the somite last, or the zones of most intense *Pax-1* expression are more resistant to the lack of notochordal signals. In any case, both markers remain constantly separated, indicating that the entire set is shifted as a whole.

The distribution of the *Pax-1* transcript anticipates the later observed vertebral phenotype. Minor *Pax-1* reduction corresponds to vertebral bodies reduced in anteroposterior dimension, more prominent at the caudal border of individual vertebrae. Either the very ventromedial identity is already lost or a diminished amount of a functional *Pax-1* product fails to confer anteroposterior differentiation to the medial sclerotome as observed in the *Pax-1* mutant undulated extensive (S. Dietrich, unpublished). Restriction of *Pax-1* expression to the lateral portion of the sclerotome, the prospective anlage of the rib and the pedicle (Töndury and Theiler, 1990), correlates with the absence of the vertebral bodies. Located in the caudal portion of the segment, the remaining *Pax-1* product might fail to guide anteroposterior differentiation, explaining the fusion of adjacent vertebral rudiments. This interpretation is supported by notochord removal experiments in amphibian neurulae and chicken, where the formation of an unsegmented cartilage tube surrounding the spinal cord has been observed (Kitchin, 1949; Teillet and Le Douarin, 1983; Theiler, 1950). Last, the *Pax-1* gene is not expressed at all; no sclerotome and subsequently no vertebral column develops, suggesting that *Pax-1* expression is required for the development of the axial skeleton.

Interestingly, in *Pt* animals and *Sd/+* heterozygotes one focus of vertebral malformations is the lumbosacral region, like in the undulated mutation (Grüneberg, 1963). Since in this region the largest vertebrae are formed, the phenotype may indicate a larger quantitative requirement for the *Pax-1* gene product, insufficiently supplied due to the notochord degeneration in the former, and the mutation in the *Pax-1* gene itself (Balling et al., 1988) in the latter.

Expanded Pax-3 expression indicates dorsalisation of the neural tube

The regional specification of the neuroectoderm closely resembles the events in the paraxial mesoderm. To the loss of the notochord both tissues respond by a similar ventral shift of a whole set of dorsoventral markers (Goulding et al., 1993, Fig. 10B). However, while *Pax-3* initially is expressed all over in the somite, the staining in the neural tube is always restricted to the dorsal aspect. This dorsal part of the neural tube therefore appears to be specified early, presumably by a dorsalising signal (Basler et al., 1993; Teillet and Le Douarin, 1983). Due to the lack of appropriate markers, the status of the ventral portion is unclear. Lacking *Pax-3* staining however, it cannot be dorsally predisposed. Initial notochordal absence leads to dorsalisation of the neuroectoderm, as indicated by the ventromedial expansion of the *Pax-3* domain or even the development of a ventral, unpaired spinal ganglion in amphibia (e.g. Kitchin, 1949). Dorsalisation is also caused by later notochord degeneration, then preceding the dorsalisation observed in the somite. Just before the floor plate can be identified morphologically, the neural tube becomes less permissive to respecification, as the *Pax-3* expression after notochord ablation does not reach the ventral midline any longer (Goulding et al., 1993). This indicates the first sign of ventral commitment. After the floor plate is established, the neural tube is as invariant to notochord alterations as the somite.

Model: Two functions of the notochord in the dorsoventral patterning of the paraxial mesoderm

Summarising our data we propose the following model for the dorsoventral patterning of the paraxial mesoderm in the mouse (Fig. 10): when the somite

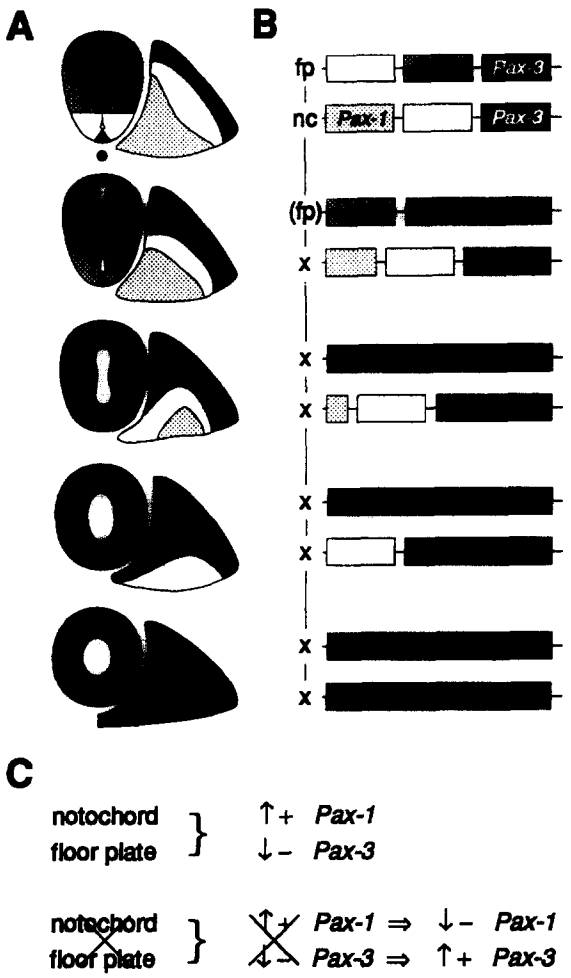

Fig. 10. Model for the dorsoventral differentiation of the paraxial mesoderm (A) Schematic representation of marker gene expression in wildtype and notochord mutant mice; *Pax-6* domain according to (Goulding et al., 1993). In the wildtype animals, the notochord ventralises neural tube and somite, inducing the floor plate, activating *Pax-1* and repressing *Pax-3*. In the mutants, ventral identity is reduced, the more exteme the earlier the notochord vanishes with respect to the state of neural tube and somite differentiation. (B) Distance between *Pax* gene expression domains and midline. Reduction or loss of the ventralising signal results in the shift of the entire set of marker genes. (C) Summary: patterning of the paraxial mesoderm by the notochord/ floor plate. Notochord/ floor plate influence activates *Pax-1* and represses *Pax-3*. When this influence is abolished, *Pax-1* expression cannot be initiated and maintained. Since repression of *Pax-3* fails, the gene is transcribed throughout.

detaches from the presomitic mesoderm, it may already be dorsally predisposed, as indicated by the overall expression of the *Pax-3* gene. The dorsal lineage may represent the default pathway for somitic cells, and may have been induced earlier by a dorsalising signal (Basler et al., 1993; Teillet and Le Douarin, 1983). Responding to an instructive induction through the notochord, *Pax-1* starts to be transcribed in the ventromedial portion of the still epithelialised somite, labelling the sclerotomal lineage. In parallel, while getting more intense the *Pax-3* signal is forced back dorsolaterally to the developing dermomyotome. Subsequently, notochord or floor plate are required over some time to maintain the dorsoventral organisation in the somite. Once the floor plate is established, the notochord is no longer necessary. Either the ventral cells are already determined to the sclerotomal lineage, or the floor plate balances the dorsalising influence. In summary, the notochord serves two functions during the dorsoventral patterning of the paraxial mesoderm: first it induces ventral identity in the somite, later it is required to maintain the specification of the sclerotomal lineage.

Experimental Procedures

Animals

Wildtype control animals were obtained by breeding of NMRI females with B6D2 males. Both parental lines are derived from the Zentralinstitut für Versuchstierzucht, Hannover. $T^c/+$ and $Pt/+$ mice were kindly provided by R. Balling, Freiburg, Germany and outcrossed for 2 generations with NMRI females. Heterozygous $Pt/+$ descendants were mated inter se, the offspring genotyped by crossing to wildtype animals, and Pt/Pt homozygous lines established. $Sd/+$ mutants are derived from the Jackson Laboratory, Bar Harbor, ME, USA. RSV/Le animals were outcrossed to NMRI and C57BL/6 (Zentralinstitut für Versuchstierzucht, Hannover, Germany). The latter revealed the milder phenotype of the C57BL/6By-*ReSdVa* line, which we kept on a C57BL/6 background. In this study, *Sd* animals without further designation belong to the NMRI line. *Truncate* animals also originate from the Jackson laboratory. Brother–sister matings were performed for 3 generations.

To correlate gene expression with developmental age, timed matings of the wildtype animals were performed for 2 h, the presence of a vaginal plug indicating day 0.0 pc. Mutant mice were mated over night, taking 12 am of the morning of the vaginal plug as day 0.5 pc. The age of the mutant litters was determined comparing external shape and *Pax* gene expression pattern to the wildtype controls.

Materials and methods

Skeletal preparations

Skeletal preparations were performed according to (Kessel et al., 1990). To photograph the vertebral column ventrally, internal organs were removed.

Whole mount in situ hybridisation

The *Pax-1* expression pattern was analysed using the paired box antisense probe described in (Deutsch et

al., 1988) and a 163 basepairs further 3' located *Sma*I antisense cDNA probe encompassing 488 nucleotides. No differences in staining were observed. The *Pax-3* antisense probe corresponds to the one utilised in (Goulding et al., 1991). The *T* antisense probe is described in (Herrmann, 1991) and was kindly provided by the author.

The whole mount in situ hybridisation procedure was performed according to (Wilkinson, 1992) using the Boehringer Digoxygenin system. The Proteinase K treatment lasted 5 min for day 8.0–9.5 pc embryos, and 15 min for older specimen. After hybridisation with the riboprobe and the anti-DIG antibody, embryos were washed over night. The staining of the animals was stopped with PBT after the wildtype pattern was reached in the anterior axial skeleton and the nonaxial expression domains. To quantitavely register the expression pattern in the four mutants, the labelled segments were counted, the average calculated and compared to the average total somite number.

Sections

Embryos up to stage 9.5 pc were embedded in Paraplast plus according to (Kaufman, 1992) and sectioned to 8 μm on a Reichert-Jung 2040 microtome. Older animals were embedded in gelatin/albumin and sectioned to 30 μm on a Pelco 101 vibratome. All sections were collected on gelatinised slides and covered with Eukitt (Kindler) or Mowiol (Hoechst).

Microscopy

The embryonic skeletons and whole mount embryos were photographed on a Zeiss Stemi SV8 binocular microscope. Embryos younger than day 10.5 pc and the tissue sections were photographed on a Zeiss Axiophot microscope using differential interference contrast or brightfield.

Acknowledgements

We wish to thank Fabienne Pituello, Patrick Tremblay and Michael Kessel for critically reading the manuscript and for many inspiring discussions. We also thank Bernhard Herrmann for providing the *T* probe and Rudi Balling for the original *Pintail* and *Brachyury curtailed* stud males. S.D. was supported by the Deutsche Forschungsgemeinschaft and F.R.S by the Max-Planck-Gesellschaft.

References

Auerbach, R. (1954) J. Exp. Zool. 127, 305–329.
Balling, R., Deutsch, U. and Gruss, P. (1988) Cell 55, 531–535.
Basler, K., Edlund, T., Jessell, T.M. and Yamada, T. (1993) Cell 73, 687–702.
Berry, R.J. (1960) Genet. Res. 1, 439–451.
Bovolenta, P. and Dodd, J. (1991) Development 113, 625–639.
Chesley, P. (1935) J. exp. Zool. 70, 429–459.
Deutsch, U., Dressler, G.R. and Gruss, P. (1988) Cell 53, 617–625.
Gluecksohn-Schoenheimer, S. (1944) Proc. Natl. Acad. Sci. USA 30, 134–140.
Gluecksohn-Schoenheimer, S. (1945) Genetics 30, 29–38.
Goulding, M.D., Chalepkis, G., Deutsch, U., Erselius, J.R. and Gruss, P. (1991) EMBO J. 10, 1135–1147.
Goulding, M.D., Lumsden, A. and Gruss, P. (1993) Development 117, 1001–1016.
Griffith, C.M., Wiley, M.J. and Sanders, E.J. (1992) Anat. Embryol. 185, 101–113.
Grüneberg, H. (1953) J. Genet. 51, 317–326.
Grüneberg, H. (1963) The Pathology of Development. Blackwell Scientific: Oxford.
Herrmann, B.G. (1991) Development 113, 913–917.
Kaufman, M. (1992) The Atlas of Mouse Development. Academic Press: New York.
Kessel, M., Balling, R. and Gruss, P. (1990) Cell 61, 301–308.
Kessel, M. and Gruss, P. (1991) Cell 67, 89–104.
Kitchin, I.C. (1949) J. Exp. Zool. 112, 393–415.
Maulbecker, C.C. and Gruss, P. (1993) EMBO J. 12, 2361–2367.
Ordahl, C.P. and Le Dourain, N.M. (1992) Development 114, 339–353.
Paavola, L.G., Wilson, D.B. and Center, E.M. (1980) J. Embryol. Exp. Morphol. 55, 227–245.
Placzek, M., Tessier-Lavigne, M., Yamada, T., Jessel, T. and Dodd, D. (1990) Science 250, 985–988.
Pourquié, O., Coltey, M., Teillet, M.-A., Ordahl, C. and Le Douarin, N.M. (1993) Proc. Natl. Acad. Sci. USA 90, 5242–5246.
Searle, A.G. (1966) Genet. Res. 7, 86–95.
Teillet, M.-A. and Le Douarin, N.M. (1983) Dev. Biol. 98, 192–211.
Theiler, K. (1950) Roux' Arch. Entw. Mech. 144, 476–490.
Theiler, K. (1959) Am. J. Anat. 104, 319–343.
Töndury, G. and Theiler, K. (1990) Entwicklungsgeschichte und Fehlbildungen der Wirbelsäule. Hippokrates Verlag: Stuttgart.
van Straaten, H.W.M., Thors, F., Wiertz-Hoessels, E.L. and Drukker, J. (1985) Dev. Biol. 110, 247–254.
Wilkinson, D.G. (1992) In Situ Hybridisation; A Practical Approach. Oxford UP: London.
Wilkinson, D.G., Bhatt, S. and Herrmann, B.G. (1990) Nature 343, 657–659.
Wilson, V., Rashbass, P. and Beddington, R.S.P. (1993) Development 117, 1321–1331.
Wright, M.E. (1947) Heredity 1, 137–141.
Yamada, T., Placzek, M., Tanaka, H., Dodd, J. and Jessell, T.M. (1991) Cell 64, 635–647.

Note added in proof

After submission of this manuscript two articles related to this study have been published that describe (a) an ectopic *Pax-1* expression following the transplantation of an additional notochord (B. Brand-Saberi et al., Anat. Embryol. 188, 239–245) and (b) the altered expression of *Pax-1* in the *Danforth's short tail* mutant (H. Koseki et al., Development 119, 649–660).